Korean J. Chem. Eng., 34(3), 692-700 (2017)
DOI: 10.1007/s11814-016-0344-7

pISSN: 0256-1115
eISSN: 1975-7220

Preparation of Cu-MgO catalysts with different copper precursors and precipitating agents for the vapor-phase hydrogenation of furfural

Samahe Sadjadi*,, Vahid Farzaneh**,***, Samira Shirvani**,***, and Mohammad Ghashghaee**,***,†**

*Gas Conversion Department, Faculty of Petrochemicals, Iran Polymer and Petrochemical Institute, P. O. Box 14975-112, Tehran, Iran
**Biomass Conversion Science and Technology (BCST) Division, Iran Polymer and Petrochemical Institute, P. O. Box 14975-115, Tehran, Iran
***Faculty of Petrochemicals, Iran Polymer and Petrochemical Institute, P. O. Box 14975-112, Tehran, Iran
(*Received 26 August 2016 • accepted 29 November 2016*)

Abstract−This article presents the effects of three copper precursors and four precipitating agents on the catalytic performance of the corresponding co-precipitated Cu-MgO catalysts in the vapor-phase hydrogenation of furfural. The chemical and physical properties were analyzed by means of XRD, BET, SEM, and EDX techniques. The nitrate precursor provided the highest performance (conversion of ~89%). Whereas, the catalyst prepared with NaOH was the most efficient (furfuryl alcohol yield of >90%) during 240 min; the most durable conversion (~95%) was assured with Na_2CO_3, and the highest selectivity to furfuryl alcohol (>97%) was achieved with K_2CO_3 as the precipitating agent. The least efficient catalyst (prepared with ammonium carbonate) led to 5-methylfurfural and 2,2-methylenebisfuran as the main byproducts. The major byproducts over the rest of the catalysts included tetrahydrofurfuryl alcohol, furfuryl ether, 1-pentanol, and 2-methylfuran. An increasing trend of furfuryl alcohol selectivity with time-on-stream was evident for all of the catalysts.

Keywords: Hydrogenation, Furfural, Furfuryl Alcohol, Cu-MgO Catalysts, Precursor, Precipitating Agent

INTRODUCTION

Depletion of the crude oil reserves, along with population growth and increasing global energy demand, as well as environmental concerns, have motivated the use of renewable resources as alternatives to fossil fuels. In this regard, biomass-derived chemicals and fuels have attracted much attention [1-5]. Furfural (dehyde), a value-added biomass-derived molecule, has been considered as a promising platform chemical [6] that can be converted into valuable fuels and products such as linear alkanes, furoic acid, 2-methylfuran, maleic acid, furan, tetrahydrofurfuryl alcohol, furfurylamine, 1,5-pentanediol, 2-methyl tetrahydrofuran, cyclopentanone, and mainly furfuryl alcohol [3,7-14]. Furfuryl alcohol that can be obtained from catalytic hydrogenation of furfural has a wide range of applications in both organic synthesis and polymer industry. The utility of furfuryl alcohol for the manufacture of foundry, liquid, and thermostatic resins, furan fiber-reinforced plastics, adhesives and farm chemicals has been proved. Moreover, as a chemical intermediate, it is used for the production of lubricants, ascorbic acid, dispersing agents, and lysine [9,15]. Hydrogenation of furfural can be carried out either in liquid [4,9,16-18] or gas phase [15,19,20]. However, the gas-phase process can be performed under milder reaction conditions, i.e., lower temperatures and H_2 pressures, or even at ambient pressure [13]. In industry, the gas-phase process is promoted by the commercial copper chromite catalyst at pressures up to 30 bar and temperatures ranging between 403 and 473 K [21]. Despite the high selectivity of copper chromate to furfuryl alcohol, the activity of the catalyst is moderate. Moreover, the use of the highly toxic chromium oxides can cause severe environmental pollution upon disposal. To circumvent these problems, a variety of alternative Cr-free mono metallic and bimetallic [22] precious and non-precious catalysts, including Cu [23], Fe [24], Pt [25,26], Ni [27], Pd, Co, Ru, and Ir supported on a relatively inert material such as silica and alumina, have been developed [28-33]. The main drawbacks of these catalysts are difficulties in recovery and reuse and fast deactivation. Among various reported catalysts, Cu-based catalysts are the most employed due to their high activity, selectivity and low cost [13]. For instance, the Cu-MgO system has received a great deal of interest for the gas-phase hydrogenation of furfural [15,32,34-37]. In spite of the promising results obtained over this catalyst, very little attention has been given to the effect of precursors. Our purpose here, then, was to study the catalytic performance of the Cu-MgO catalysts prepared via co-precipitation method with different Cu precursors in the selective conversion of furfural to furfuryl alcohol. The most efficient catalyst was further explored through varying the precipitating agent during preparation. These two factors are investigated for the first time in this paper.

EXPERIMENTAL

1. Materials

All chemicals employed for the synthesis of the catalysts were

†To whom correspondence should be addressed.
E-mail: m.ghashghaee@ippi.ac.ir, ghashghaee.m@gmail.com

used directly without any further purification after the purchase. $Cu(NO_3)_2{\cdot}3H_2O$ (99.5%), $CuSO_4{\cdot}3H_2O$ (99%), $Mg(NO_3)_2{\cdot}6H_2O$ (ACS reagent, 99%), K_2CO_3 (ACS reagent, 99.5%), NaOH (ACS reagent, 98%), $(NH_4)_2CO_3$ (Assay (acidimetric, NH_3) ≥30.0%), and Na_2CO_3 (99.9%) were purchased from Merck. $Cu(OAc)_2{\cdot}3H_2O$ (95%) was provided from Samchun Chemical Co. Ltd. The material used for the catalytic reactions included furfural (98.9%, Merck) and high purity hydrogen (99.99%) and nitrogen (99.99%).

2. Catalyst Preparation

The Cu-MgO catalysts were prepared with the percentage weight ratio of 16 : 84 for Cu : MgO through a facile co-precipitation method. In a typical procedure, a mixture of 1 M solution of copper precursor and $Mg(NO_3)_2{\cdot}6H_2O$ was precipitated at a pH of 9.0 by slow addition of 1 M aqueous solution of K_2CO_3 at ambient temperature. The mixture was then stirred vigorously for 3 h. The obtained precipitate was filtered and washed several times with distilled water and subsequently dried at 393 K for 15 h. The dried sample was then calcined in air at 723 K for 5 h with a heating rate of 5 $Kmin^{-1}$. The catalysts prepared from $Cu(NO_3)_2{\cdot}3H_2O$, $CuSO_4{\cdot}3H_2O$ and $Cu(OAc)_2{\cdot}3H_2O$ copper precursors were denoted as CM1, CM2, and CM3, respectively. Three other catalysts were also synthesized according to the above-mentioned procedure for CM1 except that the precipitating agents of NaOH, $(NH_4)_2CO_3$, and Na_2CO_3 were employed and the catalysts were named as CM4, CM5, and CM6, respectively.

3. Catalyst and Products Characterization

The synthesized catalysts were characterized by using SEM/EDX, BET, and XRD techniques. The SEM/EDX images of the catalysts were taken by a Tescan instrument, using Au-coated samples with an acceleration voltage of 20 kV. Room temperature powder X-ray diffraction patterns were collected using a Siemens, D5000. Cobalt Co Kα radiation was used from a sealed tube. Data were collected in the 2θ range of 10-88° with a step size of 0.02° and an exposure time of 2 s per step. BET surface areas were determined via nitrogen physisorption using a Quantachrome Chem-BET 3000 sorption analyzer (Micromeritics) at 77 K. The samples were degassed at 393 K for 3 h prior to the measurements. The liquid components leaving the reactor were collected in a condenser and taken every few minutes for analysis on a gas chromatograph (GC) equipped with a capillary column and an FID. The designation of the peaks was made by analysis on an Agilent 6890 series GC system equipped with an Agilent 5973 network mass selective detector. The device contained an HP-5ms column of 30 m×0.25 mm ID and 0.25 μm film thickness.

4. Catalytic Activity

Catalytic hydrogenation of furfural (FF) was in a quartz tubular reactor of 10-mm internal diameter. The catalyst pellets (0.3-1.0 mm) were loaded in the center of the reactor between two plugs of quartz wool. Prior to the reactions, the catalyst was reduced in a diluted flow of hydrogen (33 vol%) in nitrogen with a total flow rate of 6.42 $Lg^{-1}h^{-1}$ at 523 K for 3 h. An electrical furnace was used to supply the required energy, the temperature of which was maintained by two thermocouples and two programmable temperature controllers. The catalyst was cooled to the reaction temperature in pure hydrogen, and then furfural was injected into the reactor using a micro-feeder pump. The reactions were carried out at 453 K and WHSV of 1.7 h^{-1} under atmospheric pressure with an H_2/FF volumetric ratio of 10.

RESULTS AND DISCUSSION

To investigate the role of copper precursor in the catalytic activity for the production of furfuryl alcohol (FFA), three catalysts, CM1, CM2, and CM3, were synthesized, respectively, using copper nitrate, copper sulfate and copper acetate as copper salts under the same synthetic conditions. Fig. 1 demonstrates the effect of copper precursor on the catalytic performance of the Cu-MgO catalysts after 60 min and 240 min of operation. The conversion level and FFA selectivity remained above 82% and 96% over a 240-min period, indicating the satisfactory performance of the three catalysts. However, the CM1 sample (with the conversion of ~89% and FFA selectivity of over 97% after 240 min) was slightly superior in terms of a sustained selective conversion of furfural to furfuryl alcohol. Moreover, the durability of the CM1 catalyst with respect

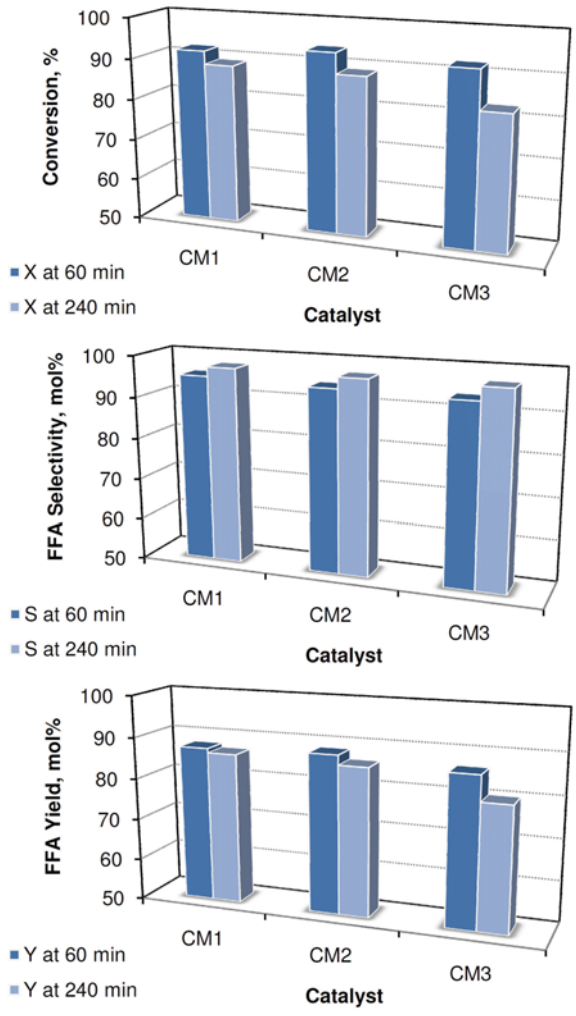

Fig. 1. Effect of copper precursor on the catalytic performance of Cu-MgO catalysts in the selective hydrogenation FF to FFA (X denotes conversion, S refers to selectivity, and Y is yield). The reaction conditions were 453 K, 1 atm, WHSV of 1.7 h^{-1}, and H_2/FF of 10.

to the FFA yield was slightly higher, keeping above 86.5% during the 240-min of operation (Fig. 1). Hence, the CM1 catalyst underwent further investigation in which the precipitating agent was altered (*vide infra*). Among the three catalysts, CM3 was the poorest; although remaining selective to FFA, CM3 experienced a gradual deactivation with time-on-stream. Lu et al. [38] demonstrated analogously that copper catalyst prepared from a nitrate source performed slightly better than that from an acetate precursor in oxidation of toluene. The same conclusion was drawn by Pachamuthu et al. [39] for the hydroxylation of phenol over a copper-grafted mesoporous material.

The synthesized catalysts demonstrated a mild increasing trend for the selectivity to FFA with time. This upward trend was concurrent with a decrease in the selectivities of other products. Fig. 2 depicts the trends of the major byproducts obtained during the reactions on the catalysts investigated. As implied from these plots, the main reaction pathways that reduce the FFA selectivity were those leading to tetrahydrofurfuryl alcohol (THFA) and 1-pentanol (1POL) for all of the catalysts. The former byproduct is formed through hydrogenation of the aromatic furan ring of furfuryl alcohol and the latter consumes FFA through a sequence of reactions involving hydrogenative dehydration of FFA to 2-methylfuran (MF), hydrogenative decyclization of MF to 2-pentanone (2PON), hydrogenation of 2PON to 2-pentanol (2POL), and the subsequent isomerization to 1POL. However, the catalysts produced also furfuryl ether (FFE) as a major byproduct, which is obtained from an etherification of two furfuryl alcohol molecules. CM3 gave MF in excess of those of the other two samples. Overall, one can speculate that the reactions leading to these compounds were suppressed and the active sites involved in these reactions were gradually covered or changed with time-on-stream, thus leading to higher selectivities to FFA. This loss in/coverage of the active centers was not very detrimental to the yield of FFA, however, particularly for the CM1 catalyst (see Fig. 1).

Other important byproducts included 2-methyltetrahydrofuran (MTHF), 2,3-dihydro-5-methylfuran (DHMF), 2-acetylfuran (AF), 1,2-pentanediol (12PDO), 5-methylfurfuryl alcohol (MFFA), γ-valerolactone (GVL), and δ-valerolactone (DVL) as shown in Fig. 3. As can be seen, CM2 produced the highest amount of THFA, while CM3 had the highest selectivities to 1POL and MF. Instead, the highest selectivity to FFE belonged to CM1.

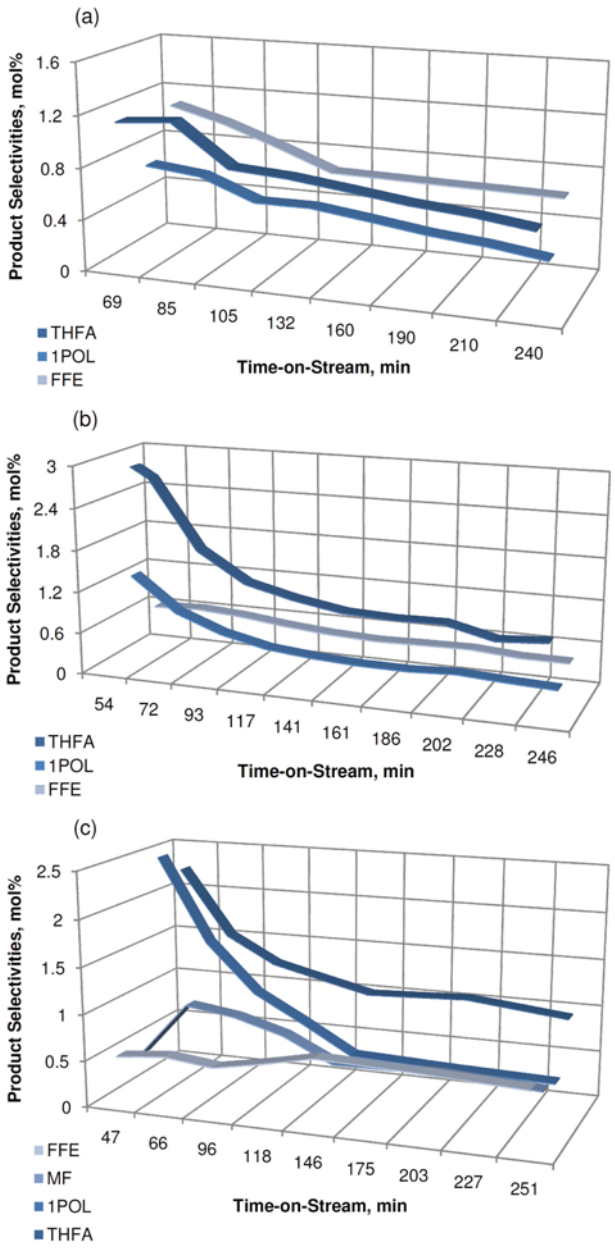

Fig. 2. The major byproducts of (a) CM1, (b) CM2, and (c) CM3. The reaction conditions were 453 K, 1 atm, WHSV of 1.7 h^{-1}, and H_2/FF of 10.

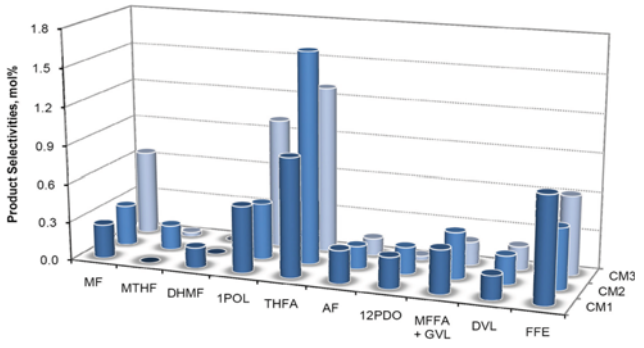

Fig. 3. Average selectivities of byproducts obtained on the Cu-MgO catalysts prepared with different copper precursors.

Table 1. Textural properties of the Cu-MgO catalysts with different copper precursors and precipitating agents

Sample	CuO crystallite size (nm)	Surface area (m^2g^{-1})	Pore volume (cm^3g^{-1})
CM1	6.2	102.26	0.35
CM2	3.4	144.29	0.53
CM3	5.5	115.33	0.45
CM4	10.6	19.97	0.30
CM5	-	168.68	0.19
CM6	9.3	51.76	0.38

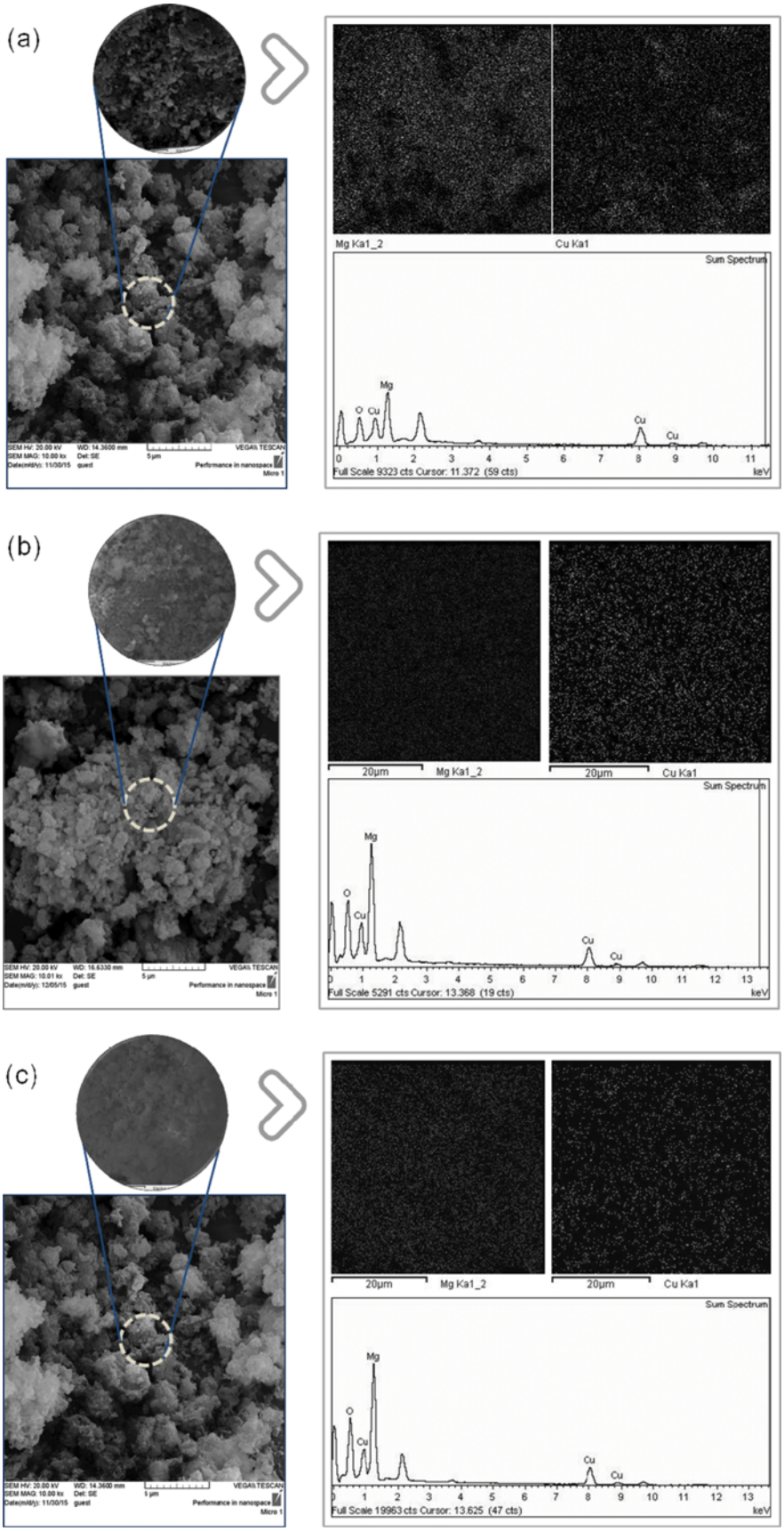

Fig. 4. SEM/EDX and elemental mapping analyses of the Cu-MgO catalysts prepared from different Cu precursors: (a) CM1, (b) CM2, and (c) CM3.

To give more insight into the origin of the different behaviors of the three catalysts, they were characterized and compared by using XRD, SEM/EDX, BET techniques. The BET surface areas of the three catalysts are tabulated in Table 1. As is obvious, CM2 had the highest surface area (144.29 m^2g^{-1}) followed by CM3 (115.33 m^2g^{-1}) and CM1 (102.26 m^2g^{-1}). Based on these results, it can be concluded that altering the copper precursor can affect the BET surface areas of the final catalyst. To provide an explanation to this observation, the morphologies of three samples were studied by using SEM technique (Fig. 4). All samples showed an aggregate-like morphology. However, the SEM images of CM1 and CM3 samples, which possessed close BET surface areas were more similar and the degree of compactness in the case of CM2 which showed the highest BET surface area was higher. Considering the fact that CM1 which has the lowest BET surface area exhibited the best catalytic performance, it can be assumed that BET surface area may not be the (only) determining factor affecting the catalytic activity. More investigation on the effects of copper precursors on the structural properties of the catalyst was carried out by using elemental mapping and EDX analyses (Fig. 4). The presence of the Cu, Mg and O elements in the EDX analyses of all samples indicated the possible formation of Cu-MgO catalysts. The elemental mapping of active species (Fig. 4) established that in CM1 sample which showed the best catalytic activity, the abundance of the active sites is superior to those of two other samples. In CM2 and CM3 samples the dispersion and abundance of Mg species are almost similar and slightly lower than CM1. The abundance and dispersion of Cu species, however, in CM3 sample which exhibited the lowest catalytic activity, was the poorest. Further details on the quality of Cu dispersion can be obtained by more specified techniques, such as N_2O chemisorption with in situ reduction [40].

The XRD patterns of the three catalysts are illustrated in Fig. 5. The position and relative intensities of all peaks confirm well with the standard patterns of MgO (JCPDS card No. 45-0946) and CuO (JCPDS card No. 05-0661 and 78-0428). The MgO phase also coincided a with probable $Mg_{0.9}Cu_{0.1}O$ phase, however. The measured CuO crystallite sizes of the three catalysts (Table 1) demonstrated that sample CM2 had the smallest CuO crystallite size (3.4 nm).

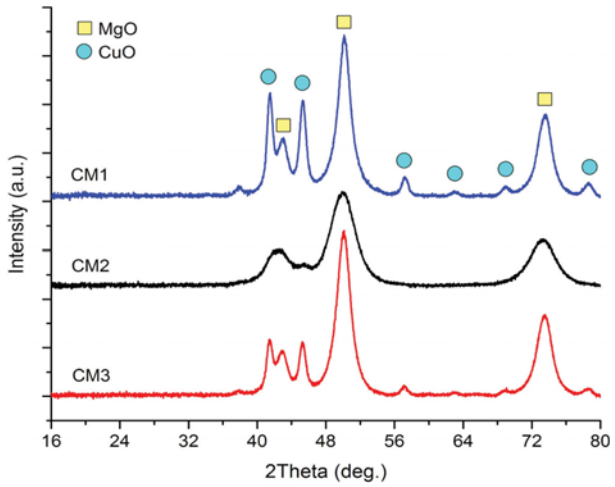

Fig. 5. The XRD patterns of CM1, CM2, and CM3.

This observation can be attributed to the high BET surface area of CM2. The largest CuO crystallite size observed for CM1, 6.2 nm could be assigned to the lower surface area of the catalyst as well as the abundance of active species that can provoke agglomeration of CuO. In the case of CM3 which had a BET surface area close to that of CM1, the CuO crystallite size was 5.5 nm. This can be due to lower abundance of copper species, as confirmed by EDX analysis, and consequently their better dispersion.

Fig. 6 shows the effects of the four precipitating agents on the catalytic performance of the Cu-MgO catalysts after 60 min and 240 min on stream. Three important indices are illustrated for the catalysts at 60 and 240 min of operation: the conversion of FF, selectivity towards FFA, and yield of FFA. While CM4 gave a conversion level above 96% at 60 min, the most sustainable conversion was observed on CM6 (~95%). Overall, the four catalysts followed the sequence of CM5<<CM1<CM4~CM6 in terms of activity. The selectivity to FFA varied in the order of CM5<CM6<CM4<CM1, however, with the highest selectivity to FFA of >97% obtained over

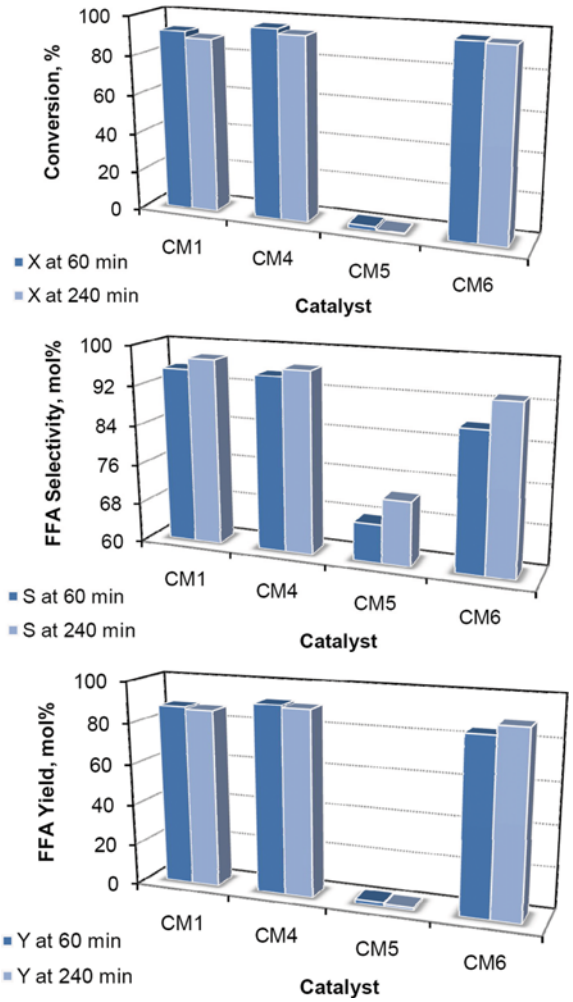

Fig. 6. Effect of precipitating agent on the catalytic performance of Cu-MgO catalysts in the selective hydrogenation of FF to FFA (X denotes conversion, S refers to selectivity, and Y is yield). The reaction conditions were 453 K, 1 atm, WHSV of 1.7 h^{-1}, and H_2/FF of 10.

CM1 at 240 min of operation. As evident in Fig. 6, all of the catalysts demonstrated increasing trends for the FFA selectivity with time, while deactivation leads to slight decreases in the conversion level during the run time.

It is obvious from Fig. 6 that CM5 with $(NH_4)_2CO_3$ as the precipitating agent had the poorest performance among the four catalysts. Although giving selectivities of up to ~73% to FFA, the amount of yield of FFA and FF conversion were almost negligible on this catalyst at the reaction conditions employed. In contrast, the other three catalysts were quite active and selective in the process. Especially, sample CM6 with Na_2CO_3 as the precipitating agent exhibited more prospects in terms of FFA production with time: a 5.3% increase in the yield of FFA during 3 h was evident for this catalyst. Nevertheless, the highest yield after 240 min of operation (above 90%) still belongs to CM4 with the NaOH used as the precipitating agent. Since the durability of CM4 is quite acceptable, this catalyst might be cautiously chosen as the best one.

Fig. 7 shows the evolution of the major byproducts on CM4, CM5, and CM6. Whereas CM4 gave THFA, MFFA, and GVL as the main byproducts, CM5 gave appreciable amounts of 5-methylfurfural (MFF) and 2,2-methylenebisfuran (MBF), and CM6 yielded THFA, MF and 1POL as the major byproducts. Indeed, the key byproducts on CM6 were most similar to those on CM1 (see Fig. 2), except that CM6 gave MF as the second byproduct and CM1 instead produced appreciable amounts of FFE. These differences point to different secondary routes of reactions on the catalysts, particularly with CM5, which was prepared with ammonium carbonate as the precipitating agent. Interestingly, it was revealed that the lack of activity was accompanied with quite different reaction pathways than on the other catalysts. In contrast to the immediate increase in the MFF selectivity, the selectivity to MBF decreased abruptly during the initial times such that MFF became the sole byproduct of this catalyst. Note, however, that the biomass-derived feedstock already contained small amounts of MFF and AF in such a manner that the observed MFF could be attributed to the unconverted impurities. Obviously, the selectivity toward FFA had an opposite trend with respect to the byproducts, not shown for the sake of brevity.

For comparison, the average selectivities of the other byproducts of the four catalysts are shown in Fig. 8. As can be seen, the selectivity to THFA varied in the order of CM5<CM1<CM4<CM6. The same sequence was observed for the case of MF and 1PDO. The next abundant byproduct, FFE, was produced in the order of CM5<CM4<CM1<CM6.

Possible interesting effects of altering the precipitating agent on the catalytic activity, selectivity and byproduct distribution motivated precise structural analyses and comparison of the catalysts prepared via different precipitating agents. The measurement of BET surface areas established that the sample prepared using $(NH_4)_2CO_3$, CM5, had the highest surface area (168.68 m^2g^{-1}) followed by CM1 (102.26 m^2g^{-1}), CM6 (51.76 m^2g^{-1}) and CM4 (19.97 m^2g^{-1}). Nevertheless, CM5 had the smallest pore volume among the catalysts investigated (Table 1). The EDX analyses of all samples showed the presence of all desired atoms, Mg, Cu and O. Studying the Mg/Cu ratio of the synthesized catalysts (Table S1), one can establish that this value was the highest on CM5 which exhibited the poorest catalytic activity. This could be the result of an aggregation of Cu

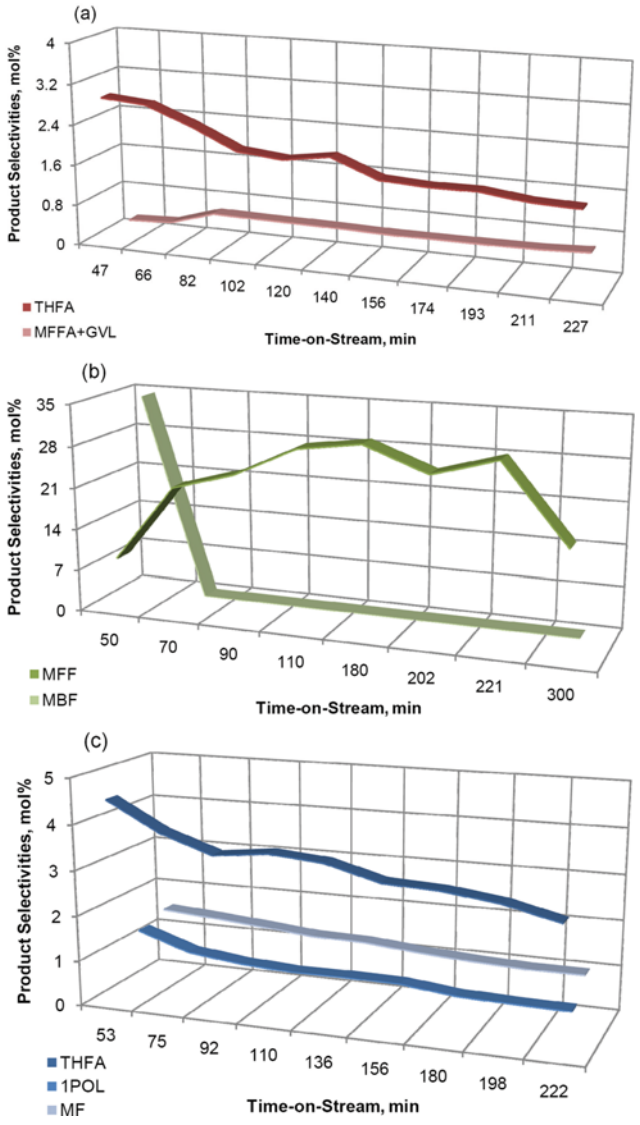

Fig. 7. The major byproducts of (a) CM4, (b) CM5, and (c) CM6. The reaction conditions were 453 K, 1 atm, WHSV of 1.7 h^{-1}, and H_2/FF of 10.

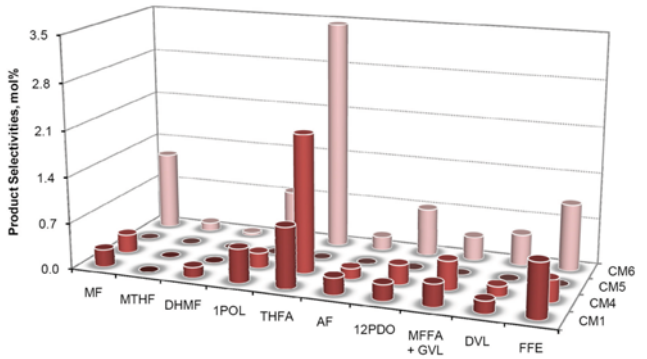

Fig. 8. Average selectivities of byproducts obtained on the Cu-MgO catalysts prepared with different precipitating agents.

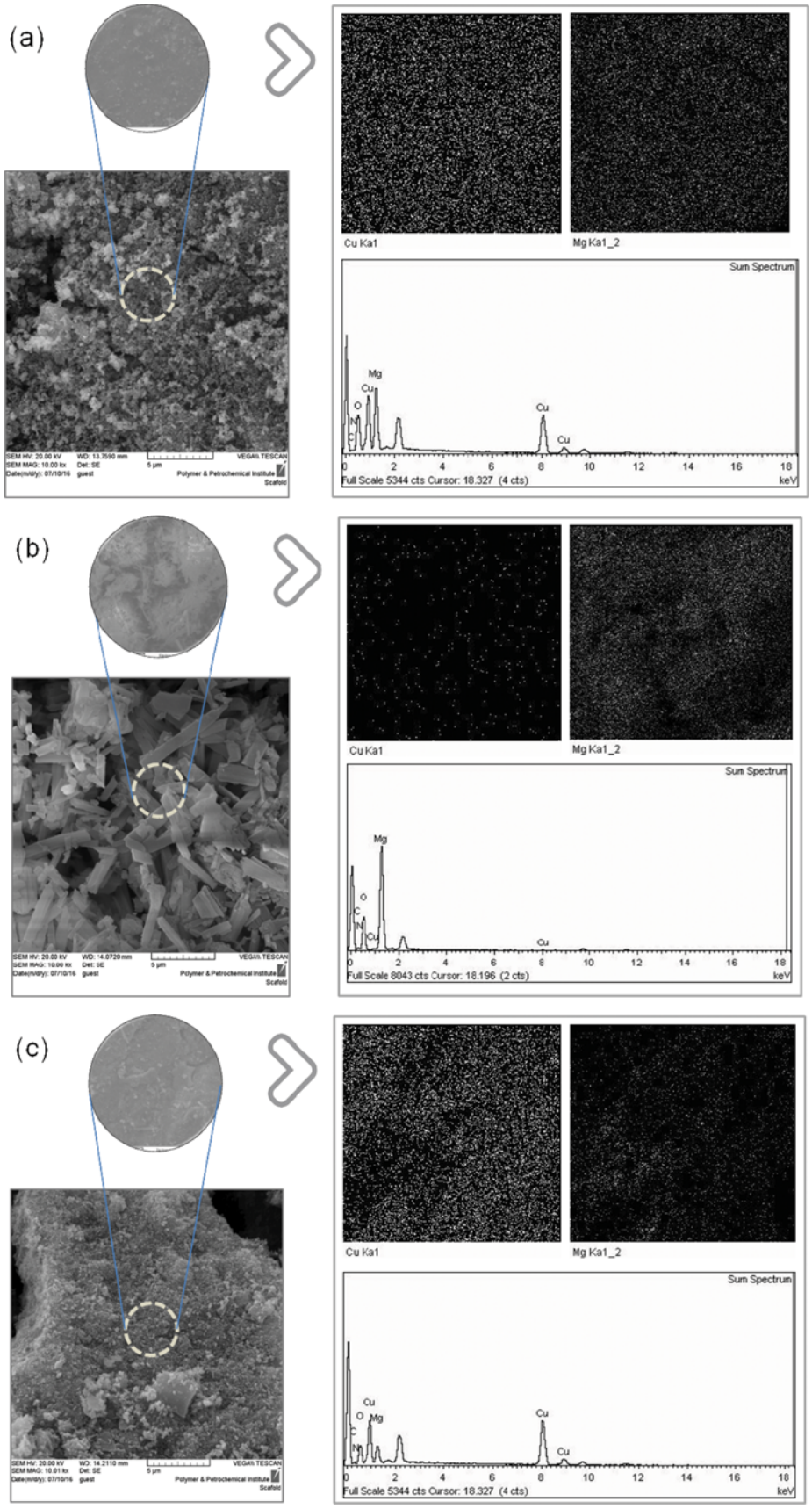

Fig. 9. SEM/EDX and elemental mapping analyses of the Cu-MgO catalysts prepared from different precipitating agents: (a) CM4, (b) CM5, and (c) CM6.

species and their serious leaching due probably to the presence of residual ammonium ions in this catalyst [41] which eventually led to its low activity. This further emphasizes the importance of the presence of Cu species on the catalyst surface for the catalytic activity. Moreover, the CM6 catalyst, which exhibited the highest activity during the run length, had the smallest value of Mg/Cu ratio, i.e., the Cu species were most abundant on the surface of this catalyst.

The SEM analysis of the samples (Fig. 9) indicated that changing the precipitating agent could affect the morphology of the final catalyst. Employing $(NH_4)_2CO_3$ as the precipitating agent led to the formation of a very distinguished rod-like morphology, which was significantly different from the other three samples. The high BET surface area observed for CM5 can be attributed to this morphology. The morphology of CM4 was almost similar to that of CM1 sample. However, the CM1 sample exhibited a more intertwined morphology. This can rationalize the higher BET surface area of CM1 compared to CM4. The elemental mapping analysis of the samples (Fig. 9) was also carried out. As is obvious, the Cu species were formed and dispersed scantily in CM5, justifying its poor catalytic performance. Comparing the elemental mapping results of CM4 and CM6 demonstrated that the Cu species are slightly more abundant in the latter.

The XRD patterns of the samples prepared by varying the precipitating agent can be seen in Fig. 10. The XRD patterns of CM4 and CM6 established the formation of the desired MgO (JCPDS card No. 45-0946) and CuO (JCPDS card No. 05-0661 and 78-0428) phases. As pointed out previously, these two catalysts (prepared respectively with NaOH and Na_2CO_3 precipitants) presented almost close performances in terms of furfural conversion despite the remarkably larger surface area of the latter. These observations are in good agreement with those reported by Huang et al. [41] for the hydrogenolysis of glycerol over Cu/SiO_2 catalysts. At the same time, the small superiority of CM6 in comparison with CM4 could be assigned to the larger size of the pores in the former (Table 1), which originated most possibly from the formation of CO_2 molecules leaving the precipitate, thus making the voids in the catalyst structure [42]. In contrast, the XRD pattern of CM5 sample is clearly different from others, mainly exhibiting the formation of an MgO-rich phase. According to the previous reports [43] and considering the results of BET and elemental analysis, this observation was attributed to the low amount of copper species.

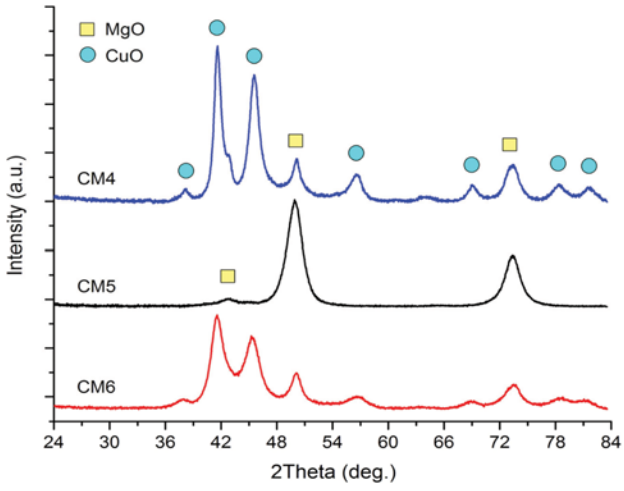

Fig. 10. The XRD patterns of (a) CM4, (b) CM5, and (c) CM6.

The calculation of the CuO crystallite sizes of the catalysts (Table 1) indicated that CM1 (6.2 nm) and CM4 (10.6 nm) had the smallest and the largest crystallite sizes, respectively. The large crystallite size of CM4 can be due to its low BET surface area. Noteworthy, the CuO crystallite size could not be calculated due to the absence of the characteristic peaks of CuO.

Finally, a comparison of the activity of the synthesized catalysts against those of the classic copper chromite catalyst for the vapor-phase hydrogenation of furfural (Table S2) can indicate the better performance of the Cu-MgO catalysts in terms of conversion of furfural, yield and selectivity of furfuryl alcohol, and particularly the catalyst durability. According to these data, the copper chromite catalysts experienced severe deactivation during the first hours of operation [44,45]. More strictly, 70% of the initial activity was lost after 4 h, most probably because of coke formation and migration of the chromite species, thus blocking the active sites of the catalyst [45]. To these should be added the absence of chromium, a toxic component, in the developed Cu-MgO catalysts.

CONCLUSION

The nitrate, sulfate, and acetate salts of Cu(II) were employed as copper precursors in the preparation of co-precipitated Cu-MgO catalysts for the selective hydrogenation of FF to FFA. The experiments at 453 K and mass-based space velocity of 1.7 h^{-1} proved that all of the catalysts were acceptably selective and active, with the nitrate precursor giving the highest performance (FF conversion of ~89%). To further explore the preparation conditions, the precipitating agent was altered for this catalyst (K_2CO_3, NaOH, $(NH_4)_2CO_3$, and Na_2CO_3), which indicated the relative favorability of all but one sample (prepared from ammonium carbonate). A mild increasing trend for the selectivity to FFA with time was apparent for all the catalysts. The reactions that reduced the selectivity to FFA were mainly those leading to THFA, FFE, 1POL, and MF. While the Cu-MgO catalyst prepared with NaOH was the most efficient (giving an FFA yield above 90%) during 240 min of operation, the most durable conversion (~95%) was achieved on CM6 (Na_2CO_3) and the highest selectivity to FFA (>97%) was obtained on CM1 (K_2CO_3). The CM5 sample with ammonium carbonate as the precipitating agent was the poorest catalyst, exhibiting appreciable amounts of MFF and MBF as the main side components. The analyses of the catalysts showed that altering the copper precursor and precipitating agent can affect the structural features of the final catalyst. All the catalysts precipitated by using K_2CO_3 showed an aggregate-like morphology. Moreover, the sample prepared from copper sulfate exhibited the highest surface area and the smallest CuO crystallite size. Testing various precipitating agents to precipitate the copper nitrate demonstrated that using NaOH led to the formation of catalyst with the lowest surface area and the largest CuO crystallite size. In the case of using $(NH_4)_2CO_3$ as the precipitating agent, a rod-like morphology, which was distinguished from others, as well as a high surface area were observed. However, the formation and dispersion of Cu species were very

poor on this catalyst, justifying its low catalytic activity.

ACKNOWLEDGEMENT

The authors appreciate the financial support from Iran Polymer and Petrochemical Institute.

SUPPORTING INFORMATION

Additional information as noted in the text. This information is available via the Internet at http://www.springer.com/chemistry/journal/11814.

REFERENCES

1. S. G. Wettstein, D. M. Alonso, E. I. Gürbüz and J. A. Dumesic, *Curr. Opin. Chem. Eng.*, **1**(3), 218 (2012).
2. K. Ulbrich, The Conversion of Furan Derivatives from Renewable Resources into valuable Building Blocks and their Application in Synthetic Chemistry, PhD Dissertation, University of Regensburg (2014).
3. C. P. Jiménez-Gómez, J. A. Cecilia, D. Durán-Martín, R. Moreno-Tost, J. Santamaría-González, J. Mérida-Robles, R. Mariscal and P. Maireles-Torres, *J. Catal.*, **336**, 107 (2016).
4. M. J. Taylor, L. J. Durndell, M. A. Isaacs, C. M. A. Parlett, K. Wilson, A. F. Lee and G. Kyriakou, *Appl. Catal. B: Environ.*, **180**, 580 (2016).
5. M. J. Climent, A. Corma and S. Iborra, *Green Chem.*, **16**(2), 516 (2014).
6. K. Yan, G. Wu, T. Lafleur and C. Jarvis, *Renew Sustainable Energy Rev.*, **38**, 663 (2014).
7. K. Yan, X. Wu, X. An and X. Xie, *Functional Mater. Lett.*, **6**(01), 1350007-1350001-1350007-1350005 (2013), DOI:10.1142/S1793604713500070.
8. H. Zhu, M. Zhou, Z. Zeng, G. Xiao and R. Xiao, *Korean J. Chem. Eng.*, **31**(4), 593 (2014).
9. Q. Yuan, D. Zhang, L. van Haandel, F. Ye, T. Xue, E. J. M. Hensen and Y. Guan, *J. Mole. Catal. A: Chem.*, **406**, 58 (2015).
10. K. Yan and A. Chen, *Fuel*, **115**, 101 (2014).
11. T. P. Sulmonetti, S. H. Pang, M. T. Claure, S. Lee, D. A. Cullen, P. K. Agrawal and C. W. Jones, *Appl. Catal., A*, **517**, 187 (2016).
12. A. Halilu, T. H. Ali, A. Y. Atta, P. Sudarsanam, S. K. Bhargava and S. B. Abd Hamid, *Energy Fuels*, **30**, 2216 (2016).
13. D. Vargas-Hernández, J. M. Rubio-Caballero, J. Santamaría-González, R. Moreno-Tost, J. M. Mérida-Robles, M. A. Pérez-Cruz, A. Jiménez-López, R. Hernández-Huesca and P. Maireles-Torres, *J. Mol. Catal. A: Chem.*, **383-384**, 106 (2014).
14. M. Manikandan, A. K. Venugopal, A. S. Nagpure, S. Chilukuri and T. Raja, *RSC Adv.*, **6**(5), 3888 (2016).
15. B. M. Nagaraja, A. H. Padmasri, B. David Raju and K. S. Rama Rao, *J. Mol. Catal. A*, **265**(1-2), 90 (2007).
16. R. V. Sharma, U. Das, R. Sammynaiken and A. K. Dalai, *Appl. Catal. A*, **454**, 127 (2013).
17. M. M. Villaverde, T. F. Garetto and A. J. Marchi, *Catal. Commun.*, **58**, 6 (2015).
18. J. Li, J.-l. Liu, H.-j. Zhou and Y. Fu, *ChemSusChem*, **9**(11), 1339 (2016).
19. M. Li, Y. Hao, F. Cárdenas-Lizana and M. A. Keane, *Catal. Commun.*, **69**, 119 (2015).
20. K. Yan and A. Chen, *Energy*, **58**, 357 (2013).
21. J. Kijeński, P. Winiarek, T. Paryjczak, A. Lewicki and A. Mikołajska, *Appl. Catal. A*, **233**(1-2), 171 (2002).
22. A. B. Merlo, V. Vetere, J. F. Ruggera and M. L. Casella, *Catal. Commun.*, **10**(13), 1665 (2009).
23. K. Yan, J. Liao, X. Wu and X. Xie, *RSC Adv.*, **3**(12), 3853 (2013).
24. H. Li, H. Luo, L. Zhuang, W. Dai and M. Qiao, *J. Mole. Catal. A: Chem.*, **203**(1-2), 267 (2003).
25. M. Lesiak, M. Binczarski, S. Karski, W. Maniukiewicz, J. Rogowski, E. Szubiakiewicz, J. Berlowska, P. Dziugan and I. Witońska, *J. Mole. Catal. A: Chem.*, **395**, 337 (2014).
26. K. An, N. Musselwhite, G. Kennedy, V. V. Pushkarev, L. Robert Baker and G. A. Somorjai, *J. Colloid Interface Sci.*, **392**, 122 (2013).
27. Y. Xu, S. Qiu, J. Long, C. Wang, J. Chang, J. Tan, Q. Liu, L. Ma, T. Wang and Q. Zhang, *RSC Adv.*, **5**(111), 91190 (2015).
28. C. Xu, L. Zheng, J. Liu and Z. Huang, *Chin. J. Chem.*, **29**(4), 691 (2011).
29. B. Zhao, M. Chen, Q. Guo and Y. Fu, *Electrochim. Acta*, **135**, 139 (2014).
30. K. Fulajtárova, T. Soták, M. Hronec, I. Vávra, E. Dobročka and M. Omastová, *Appl. Catal. A: Gen.*, **502**, 78 (2015).
31. Y. Nakagawa, K. Takada, M. Tamura and K. Tomishige, *ACS Catal.*, **4**(8), 2718 (2014).
32. B. M. Nagaraja, A. H. Padmasri, B. D. Raju and K. S. Rama Rao, *Int. J. Hydrogen Energy*, **36**(5), 3417 (2011).
33. O. F. Aldosari, S. Iqbal, P. J. Miedziak, G. L. Brett, D. R. Jones, X. Liu, J. K. Edwards, D. J. Morgan, D. K. Knight and G. J. Hutchings, *Catal. Sci. Technol.*, **6**(1), 234 (2016).
34. B. M. Nagaraja, V. S. Kumar, V. Shasikala, A. H. Padmasri, B. Sreedhar, B. D. Raju and K. S. Rao, *Catal. Commun.*, **4**(6), 287 (2003).
35. H. Cui, X. Wu, Y. Chen, J. Zhang and R. I. Boughton, *Mater. Res. Bulletin*, **61**, 511 (2015).
36. A. J. Estrup, Selective Hydrogenation of Furfural to Furfuyl Alcohol over Copper Magnesium Oxide. MSc, University of Maine (2015).
37. H. Liu, Q. Hu, G. Fan, L. Yang and F. Li, *Catal. Sci. Technol.*, **5**(8), 3960 (2015).
38. C.-Y. Lu, M.-Y. Wey and Y.-H. Fu, *Appl. Catal. A: Gen.*, **344**(1-2), 36 (2008), DOI:http://dx.doi.org/10.1016/j.apcata.2008.03.036.
39. M. P. Pachamuthu, V. V. Srinivasan, R. Maheswari, K. Shanthi and A. Ramanathan, *Catal. Sci. Technol.*, **3**(12), 3335 (2013).
40. J. R. Jensen, T. Johannessen and H. Livbjerg, *Appl. Catal. A: Gen.*, **266**(1), 117 (2004).
41. Z. Huang, H. Liu, F. Cui, J. Zuo, J. Chen and C. Xia, *Catal. Today*, **234**, 223 (2014).
42. T. R. Motjope, H. T. Dlamini, G. R. Hearne and N. J. Coville, *Catal. Today*, **71**(3), 335 (2002).
43. S. Mallik, S. S. Dash, K. M. Parida and B. K. Mohapatra, *J. Colloid Interface Sci.*, **300**(1), 237 (2006).
44. D. Liu, D. Zemlyanov, T. Wu, R. J. Lobo-Lapidus, J. A. Dumesic, J. T. Miller and C. L. Marshall, *J. Catal.*, **299**, 336 (2013).
45. H. Zhang, C. Canlas, A. J. Kropf, J. W. Elam, J. A. Dumesic and C. L. Marshall, *J. Catal.*, **326**, 172 (2015).

Supporting Information

Preparation of Cu-MgO catalysts with different copper precursors and precipitating agents for the vapor-phase hydrogenation of furfural

Samahe Sadjadi[*,], Vahid Farzaneh[**,***], Samira Shirvani[**,***], and Mohammad Ghashghaee[**,***,†]**

*Gas Conversion Department, Faculty of Petrochemicals, Iran Polymer and Petrochemical Institute, P. O. Box 14975-112, Tehran, Iran
**Biomass Conversion Science and Technology (BCST) Division, Iran Polymer and Petrochemical Institute, P. O. Box 14975-115, Tehran, Iran
***Faculty of Petrochemicals, Iran Polymer and Petrochemical Institute, P. O. Box 14975-112, Tehran, Iran
(*Received 26 August 2016 • accepted 29 November 2016*)

Table S1. The Mg/Cu weight ratio (determined from EDX data)

Sample	Mg/Cu
CM1	0.91
CM2	1.72
CM3	1.83
CM4	0.51
CM5	69.36
CM6	0.17

REFERENCES

1. D. Liu, D. Zemlyanov, T. Wu, R. J. Lobo-Lapidus, J. A. Dumesic, J. T. Miller and C. L. Marshall, *J. Catal.*, **299**, 336 (2013).
2. H. Zhang, C. Canlas, A. J. Kropf, J. W. Elam, J. A. Dumesic and C. L. Marshall, *J. Catal.*, **326**, 172 (2015).
3. R. Rao, A. Dandekar, R. T. K. Baker and M. A. Vannice, *J. Catal.*, **171**(2), 406 (1997).
4. B. M. Nagaraja, H. P. Aytam, S. Podila, K. H. P. Reddy, B. D. Raju and S. R. R. Kamaraju, *J. Mol. Catal. A*, **278**(12), 29 (2007).

Table S2. Overview of the vapor-phase hydrogenation of furfural over classic copper chromite catalysts

Catalyst	Temp. (°C)	Press. (atm)	H_2/FF ratio	Conversion (%)	Selectivity (%)	Yield (%)	Remarks	Ref.
Commercial Copper Chromite (Cu-1800P)	200	1	25	22	91.2	20.1	The conversion level decreased gradually to 10% while the selectivity reached 97% after 250 min	[1]
Commercial Copper Chromite	200	1	25	20.0	18.0	3.6	The conversion level decreased from 98.2% to 20.0% after 500 min and to 16.3% after 700 min. The tabulated values are those at the 500 min	[2]
Commercial Copper Chromite (Cu-1800P)	140	1	73	The specific activity was 0.26 μmol/(m^2·s)	70	-	Turnover frequency (TOF) was 1.05 s^{-1} based on irreversible hydrogen adsorption and 0.34 s^{-1} based on total hydrogen adsorption. The reported activity was based on furfural disappearance	[3]
Commercial Copper Chromite (Cu-1800P)	180	1	-	46	65	30	-	[4]
Cu-MgO (CM4)	180	1	10	96.1	94.9	91.2	The conversion level and yield decreased, respectively, to 93.4% and 90.1% after 240 min	This work